

# Evolution of the pseudogap temperature dependence in $\text{YBa}_2\text{Cu}_3\text{O}_{7-\delta}$ films under the influence of a magnetic field

E. V. Petrenko<sup>1</sup>, A. V. Terekhov<sup>1</sup>, L. V. Bludova<sup>1</sup>, Yu. A. Kolesnichenko<sup>1</sup>,N. V. Shytov<sup>1</sup>, D. M. Sergeyev<sup>2</sup>, E. Lähderanta<sup>3</sup>, K. Rogacki<sup>4</sup>, A. L. Solovjov<sup>1,3,4</sup><sup>1</sup>*B. Verkin Institute for Low Temperature Physics and Engineering of National Academy of Science of Ukraine, Kharkiv 61103, Ukraine*<sup>2</sup>*K. Zhubanov Aktobe Regional State University, 030000 Aktobe, Kazakhstan*<sup>3</sup>*Lappeenranta University of Technology, School of Engineering Science, 53850 Lappeenranta, Finland*<sup>4</sup>*Institute of Low Temperature and Structure Research of Polish Academy of Science, 50-422 Wrocław, Poland*

The evolution of the temperature dependence of pseudogap  $\Delta^*(T)$  in optimally doped (OD)  $\text{YBa}_2\text{Cu}_3\text{O}_{7-\delta}$  (YBCO) films with  $T_c = 88.7$  K under the influence of a magnetic field  $B$  up to 8 T has been studied in detail. It has been established that the shape of  $\Delta^*(T)$  for various  $B$  over the entire range from the pseudogap opening temperature  $T^*$  to  $T_{01}$ , below which superconducting fluctuations occur, has a wide maximum at the BEC-BCS crossover temperature  $T_{pair}$ , which is typical for OD films and untwinned YBCO single crystals.  $T^*$  was shown to be independent on  $B$ , whereas  $T_{pair}$  shifts to the low temperature region along with increase of  $B$ , while the maximum value of  $\Delta^*(T_{pair})$  remains practically constant regardless of  $B$ . It was revealed that as the field increases, the low-temperature maximum near the 3D-2D transition temperature  $T_0$  is blurred and disappears at  $B > 5$  T. Moreover, above the Ginzburg temperature  $T_G$ , which limits superconducting fluctuations from below, at  $B > 0.5$  T, a minimum appears on  $\Delta^*(T)$  at  $T_{min}$ , which becomes very pronounced with a further increase in the field. As a result, the overall value of  $\Delta^*(T)$  decreases noticeably most likely due to pair-breaking affect of a magnetic field. A comparison of  $\Delta^*(T)$  near  $T_c$  with the Peters-Bauer theory shows that the density of fluctuating Cooper pairs actually decreases from  $\langle n_{\uparrow}n_{\downarrow} \rangle \approx 0.31$  at  $B = 0$  to  $\langle n_{\uparrow}n_{\downarrow} \rangle \approx 0.28$  in the field 8 T. The observed behavior of  $\Delta^*(T)$  around  $T_{min}$  is assumed to be due to the influence of a two-dimensional vortex lattice created by the magnetic field, which prevents the formation of fluctuating Cooper pairs near  $T_c$ .

Keywords: high-temperature superconductors, YBCO films, excess conductivity, fluctuation conductivity, pseudogap, magnetic field, coherence length.

PACS numbers: 74.25.Fy, 74.72.-h, 74.72.Bk, 74.78.Fk

## 1. INTRODUCTION

The number of works devoted to high-temperature superconductors (HTSCs) keeps growing steadily, and this is not surprising: after the resonant publication of Lee *et al.* [1], interest in such materials has increased even more. Unfortunately, so far no scientific group in the world can confirm the sought-after superconductivity at normal pressure [2, 3] declared by [1] in modified lead apatite. The impossibility of synthesizing compounds with zero resistance at room temperatures and ambient pressure is primarily due to the lack of a complete understanding of the mechanism of superconducting pairing at superconducting transition temperatures above 100 K.

In addition, cuprates at some temperature range above  $T_c$  exhibit an unusual feature known as a pseudogap (PG) [4–10], which opens in lightly doped  $\text{YBa}_2\text{Cu}_3\text{O}_{7-\delta}$  (YBCO) at a characteristic temperature  $T^* \gg T_c$  [11, 12]. It is believed that studying the PG phenomenon can definitely shed light on the microscopic mechanism of high-temperature superconductivity [4, 12] (and references there in). However, the physics behind PG is still uncertain. The aforementioned YBCO cuprates, as is known, belongs to the class of metal oxides with active  $\text{CuO}_2$  planes and, in addition to high  $T_c$  and PG, have a low charge carrier density  $n_f$ , strong electronic correlations, quasi-two-dimensionality and, as a consequence, strong anisotropy of electronic properties [11, 13–15]. In particular, the coherence length along the  $ab$  plane, which determines the size of Cooper pairs in HTSCs, is  $\xi_{ab}(T) \approx 10\xi_c(T)$ , where  $\xi_c(T)$  is the coherence length along the  $c$ -axis [12].

We support an idea that a low charge carrier density,  $n_f$ , is a necessary condition for the formation of paired fermions in cuprates below the characteristic temperature  $T^* \gg T_c$ , the so-called local pairs (LPs) [14, 16], which, most likely,

responsible for the formation of the PG state ([12, 16–18] and references therein). At high temperatures  $T \leq T^*$ , LPs appear in the form of strongly bound bosons (SBBs), which obey the Bose-Einstein condensation theory (BEC) [17]. Since  $\xi_{ab}(T^*) \approx 10 \text{ \AA}$  in YBCO, SBBs are small, but very tightly bound pairs, since, according to the theory [13, 15], the binding energy in a pair  $\epsilon_B \sim 1/\xi_{ab}^2$ . As a result, SBBs are not destroyed by thermal fluctuations and any other influences. However, with decreasing temperature,  $\xi(T)$  and, consequently, the pair size increase, and the SBBs gradually transform into fluctuating Cooper pairs (FCPs), obeying the BCS theory in the range of superconducting (SC) fluctuations near  $T_c$  [16–18]. We would like to emphasize that condensation of the FCPs into the SC state is possible only from the three-dimensional (3D) state [13, 15]. Therefore, when  $\xi_c(T)$  exceeds the size  $d$  of the YBCO unit cell along the  $c$ -axis:  $\xi_c(T) > d$  near  $T_c$ , the quasi-two-dimensional (2D) state of the HTSCs always changes to the 3D state [12, 19].

Nevertheless, some other models have been proposed to explain the physics of PG, such as spin fluctuations [20], charge (CDW) [21, 22] and spin (SDW) [7, 21, 23] density waves, charge ordering (CO) ([7, 21, 24, 25] and references therein) and even pair density waves (PDW) [8, 26]. However, in spite of the fact that the interest in the PG study has noticeably increased in recent years [8, 26–29], the physics of the PG state is still not completely clear. According to the latest concepts [7, 18, 23], below  $T^*$  a rearrangement of the Fermi surface is quite possible, which largely determines the unusual properties of cuprates in the PG region. At the same time, despite the fact that the number of works devoted to the study of HTSCs and, in particular, the PG, is extremely large, there is a lack of papers studying the influence of a magnetic field on excess conductivity in cuprates. However, it is precisely the study of the influence of the magnetic field on fluctuation conductivity (FLC) and PG that can answer the question: which of the physical mechanisms of PG considered above actually takes place in cuprates?

To the best of our knowledge, the effect of magnetic field on FLC in YBCO materials has been analyzed in a fairly small number of studies so far [30–33]. However, in [30] the applied field does not exceed 1.27 T, which is too small to draw any firm conclusions. In [31] magnetic field  $B = 12 \text{ T}$  and accordingly in [32] magnetic field  $B = 9 \text{ T}$  were used. But in [31], it is reported a decrease in  $\xi_c(T)$  along with a decrease in  $T_c$  with increasing magnetic field. It is amazing, since in the traditional theory of superconductivity  $\xi \sim 1/T_c$  [34]. In addition, in both papers the authors did not show the evolution of the FLC with a magnetic field. Moreover, we are not aware of any work that has studied the effect of the magnetic field on the PG in HTSC's.

In our previous work [33], we tried to shed light on the mechanism of the influence of the magnetic field on FLC in YBCO by studying the influence of the magnetic field in the  $ab$ -plane on the resistivity  $\rho(T)$  and fluctuation conductivity  $\sigma'(T)$  of a thin YBCO film at increasing the magnetic field to 8 T. The corresponding dependences  $\sigma'(T)$  for all applied fields were carefully analyzed. As expected, at  $B = 0$ ,  $\sigma'(T)$  near  $T_c$  was described by the 3D Aslamasov-Larkin (AL) theory [35, 36] and the 2D Maki-Thompson (MT) fluctuation theory [37] above the crossover temperature  $T_0$ . However, at  $B = 3 \text{ T}$ , the MT term is completely suppressed, and above  $T_0$ ,  $\sigma'(T)$  is unexpectedly described by the 2D-AL fluctuation contribution. At the same time,  $\xi_c(0)$  abruptly increases, that is, demonstrates a rather unusual  $\xi_c(0)$  vs  $T_c$  dependence in magnetic field (Fig. 7, curve 1 in [33]). However, the evolution of the pseudogap under the influence of a magnetic field has not been studied.

In this paper, for the first time, a detailed analysis of the temperature and field dependences of the pseudogap  $\Delta^*(T, B)$  of a thin YBCO film in a magnetic field of up to 8 T was carried out, also using all the necessary parameters obtained from the analysis of fluctuation conductivity  $\sigma'(T, B)$  in the above-mentioned work. Thus, in a sense, the article is a logical continuation of our previous research [33]. It was found that at  $B = 0$  the shape of  $\Delta^*(T)$  was expectedly typical for optimally doped films [19] and non-twinned single crystals [38], but unexpectedly changed at  $B = 8 \text{ T}$ . It was found that in the range of SC fluctuations below  $T_{01}$ , the magnetic field strongly affects both the shape and the value of  $\Delta^*(T, B)$ , which can be seen by comparing the corresponding temperature dependences of the PG at different  $B$  near  $T_c$ . To gain a deeper understanding of the influence of the magnetic field on superconducting fluctuations, a comparison was made with the Peters-Bauer theory [39] and the local pair density near  $T_c$  in the film under study was estimated as a function of the applied field. A detailed discussion of the results obtained is given below.

## 2. EXPERIMENT

Epitaxial YBCO films were deposited at  $T = 770^\circ\text{C}$  and an oxygen pressure of 3 mbar at  $(\text{LaAlO}_3)_{0.3}(\text{Sr}_2\text{TaAlO}_6)_{0.7}$  substrates, as described elsewhere [40]. The thickness of deposited films,  $d \approx 100 \text{ nm}$ , was controlled by the deposition time of respective targets. X-ray analyses have shown that all samples are excellent films with the  $c$  axis perfectly oriented perpendicular to the  $\text{CuO}_2$  planes. Next, the films were lithographically patterned and chemically etched into well-defined  $2.35 \times 1.24 \text{ mm}^2$  Hall-bar structures. To perform contacts, golden wires were glued to the structure pads by using silver epoxy. Contact resistance below  $1 \text{ } \Omega$  was obtained. The main measurements included a fully computerized setup, the Quantum Design Physical Property Measurement System (PPMS-9), by using the AC

current of  $\sim 100 \mu\text{A}$  at 19 Hz. The four-point probe technique was used to measure the in-plane resistivity  $\rho_{ab}(T) = \rho(T)$ . A static magnetic field was created using a superconducting magnet. Measurements were performed up to 9 T for the field orientations parallel to the  $B \parallel ab$ .

### 3. RESULTS AND DISCUSSION

#### 3.1. Resistivity

The temperature dependence of the resistivity  $\rho(T)$  of the  $\text{YBa}_2\text{Cu}_3\text{O}_{7-\delta}$  film in the absence of an external magnetic field is shown in Fig. 1 and is typical for all underdoped cuprates. For temperature above  $T^* = 215 \text{ K}$  and up to 300 K, the  $\rho(T)$  dependence is linear with a slope  $a = d\rho/dT = 2.050 \mu\Omega \cdot \text{cm}/\text{K}$ . The slope was calculated by fitting the experimental curve using a computer and confirmed the linear behavior of  $\rho(T)$  with a mean-root-square error of  $0.009 \pm 0.002$  in the specified temperature range. The pseudogap opening temperature  $T^* \gg T_c$  was defined as a temperature at which the resistive curve deviates downward from the linearity (Fig. 1). The more precise approach to determine  $T^*$  with accuracy  $\pm 0.5 \text{ K}$  is to explore the criterion  $[\rho(T) - \rho_0]/aT = 1$  [41] (inset in Fig. 1), where, as before,  $a$  designates the slope of the extrapolated normal-state resistivity,  $\rho_N(T)$ , and  $\rho_0$  is its intercept with the Y axis. Both methods give the same  $T^* = 215 \text{ K}$ , which is typical for well-structured YBCO films with  $T_c \approx 88 \text{ K}$  and is in good agreement with literature data [19, 42].

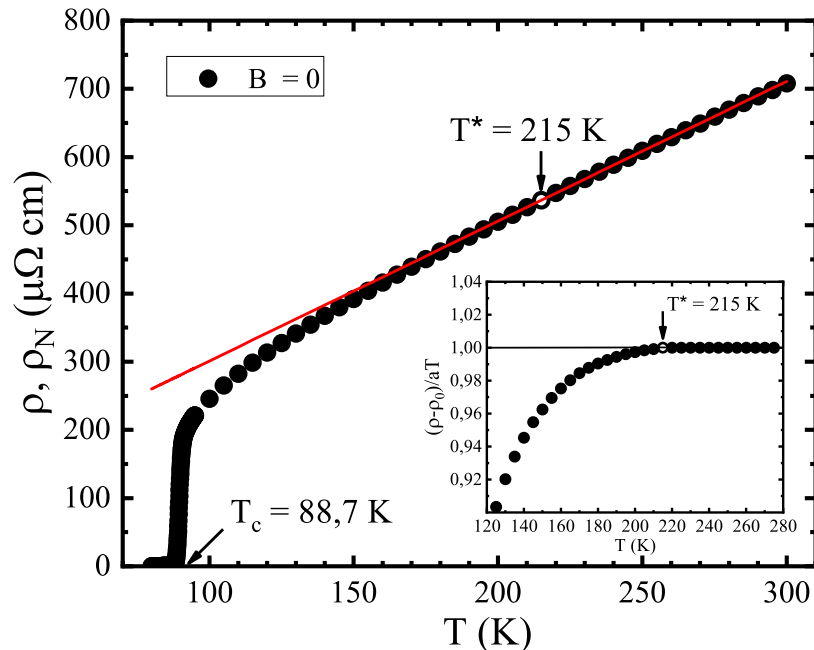


FIG. 1:  $\rho(T)$  dependence for  $\text{YBa}_2\text{Cu}_3\text{O}_{7-\delta}$  film in the absence of external magnetic field ( $B = 0$ , dots). The solid red line defines  $\rho_N(T)$ , extrapolated to the low-temperature region. The open circle corresponds to temperature  $T^*$ . Inset: method for determining  $T^*$  using criterion  $[\rho(T) - \rho_0]/aT = 1$  [41].

The influence of a magnetic field from  $B = 0$  to 8 T on the temperature dependence  $\rho(T)$  is shown in Fig. 2. As can be seen in the figure, the magnetic field noticeably broadens the resistive transition, creating magnetoresistance, and reduces  $T_c$  but, as usual, does not affect the resistivity in the normal state [43, 44]. It is worth noting the absence of any steps in SC transitions in any magnetic field, which indicates the good quality of the sample, its homogeneity, and the absence of additional phases and inclusions. Unfortunately, for the 9 T case, during the experiment, the contacts of the sample were damaged and did not allow recording the temperature dependence in this field.

#### 3.2. Excess conductivity

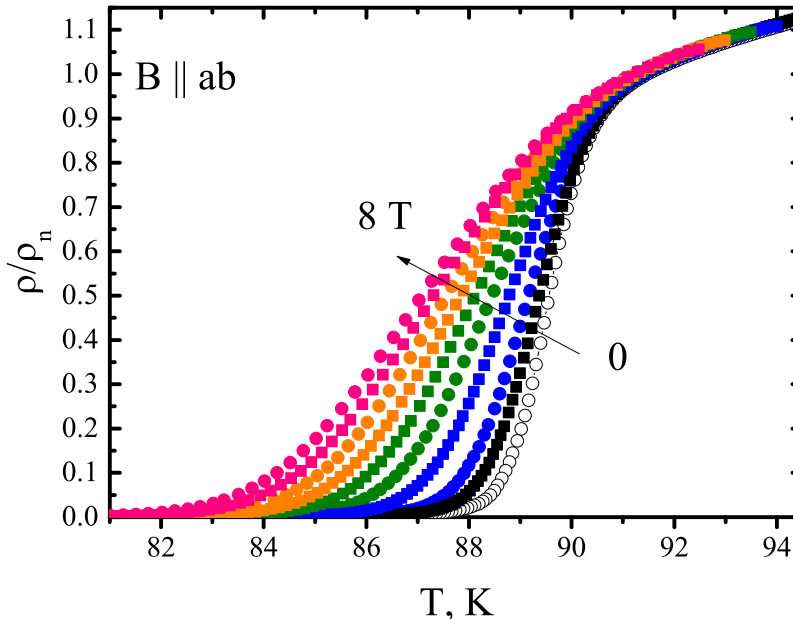


FIG. 2: Temperature dependences of  $\rho(T)$  in units of  $(\rho/\rho_n)$  of the  $\text{YBa}_2\text{Cu}_3\text{O}_{7-\delta}$  film, obtained for the field orientation parallel to the  $ab$ -plane ( $B \parallel ab$ ,  $B = 0, 0.5, 1, 2, 3, 4, 5, 6, 7$  and  $8$  T).  $\rho_n = 203 \mu\Omega\cdot\text{cm}$  at  $T = 92.3$  K is a normal state resistivity in the vicinity of the SC transition.

Below  $T^*$  (Fig. 1),  $\rho(T)$  deviates from the linear dependence toward smaller values. This leads to the appearance of excess conductivity  $\sigma'(T)$ , and the transition of HTSC to the PG state (see Refs.[12, 45, 46] and references therein). It is well known, that  $\sigma'(T)$  can be determined by the simple formula [19, 33]:

$$\sigma'(T) = \sigma(T) - \sigma_N(T) = \frac{1}{\rho(T)} - \frac{1}{\rho_N(T)} = \frac{\rho_N(T) - \rho(T)}{\rho(T) \cdot \rho_N(T)} \quad (1)$$

therefore, it is actually determined by the measured resistivity  $\rho(T)$  and the normal-state resistivity  $\rho_N(T)$  extrapolated to the low  $T$  region. This emphasizes that correctly finding  $\rho_N(T)$  is of paramount importance for determining  $\sigma'(T)$  and therefore  $\Delta^*(T)$  [12]. In cuprates,  $\rho_N(T)$  is a linear function of  $T$  over a wide temperature range above  $T^*$  [47, 48]. According to the NAFL (Nearly Antiferromagnetic Fermi-liquid) model [20], this linear dependence corresponds to the normal state of HTSCs, characterized by the stability of the Fermi surface. Below  $T^*$ , numerous anomalies of electronic properties are observed, associated with a decrease in the density of single-particle excitations and anisotropic rearrangement of the spectral density of charge carriers, most likely due to the rearrangement of the Fermi surface [7, 18, 21, 23]. Finally, within the framework of the local pair (LP) model [12], based on previously measured values of excess conductivity  $\sigma'(T)$ , the value and temperature dependence of the pseudogap parameter  $\Delta^*(T)$  was calculated for all applied magnetic fields [33].

### 3.3. Field analysis of the pseudogap

Cuprates are known to have a pseudogap (PG) that opens below  $T^*$  and leads to the appearance of excess conductivity  $\sigma'(T)$  [Eq. (1)], as mentioned above. Thus, it is believed that  $\sigma'(T)$  should contain information about the magnitude and temperature dependence of the pseudogap [49]. However, the question remains open: how to extract this information, since there is still no rigorous theory of HTSCs. As noted above, we share the idea that PG in cuprates can be associated with the formation of local pairs (LPs) at  $T < T^*$ , which at  $T \leq T^*$  appear in the form of SBBs subject to BEC, but with decreasing  $T$  they gradually change their properties to large fluctuating Cooper pairs (FCPs) near  $T_c$ , obeying the BCS theory [6, 9, 10, 12, 16–18, 49]. The classical Aslamasov-Larkin (3D-AL) [36] and Maki-Thompson (2D-MT) fluctuation theories, which were modified by Hikami and Larkin (HL) [37] for

TABLE I:  
Parameters of FLC analysis of  $\text{YBa}_2\text{Cu}_3\text{O}_{7-\delta}$  film depending on the applied magnetic field.

$B$ (T)	$T_c$ (K)	$T_c^{mf}$ (K)	$T_G$ (K)	$T_0$ (K)	$T_{01}$ (K)	$\Delta T_{fl}$ (K)	$\xi_c(0)$ (Å)
0	88.7	89.65	90.06	90.89	100.0	9.9	1.38
0.5	88.3	89.50	89.89	91.14	96.8	6.9	1.58
1	87.9	89.40	89.89	91.12	94.5	4.6	1.62
2	87.2	89.06	89.60	92.69	94.0	4.4	2.36
3	86.6	88.88	89.51	100.0	120.0	30.5	4.13
4	86.0	88.67	89.44	100.0	120.0	30.6	4.18
5	85.6	88.46	89.24	100.0	115.0	25.8	4.22
6	84.9	88.30	89.26	100.0	115.0	25.8	4.26
7	84.5	88.09	89.10	100.0	115.0	25.9	3.99
8	84.0	87.90	89.02	98.1	115.0	26.0	3.99

HTSCs, provide a good description of the experimental  $\sigma'(T)$  in cuprates, but only in the range of SC fluctuations, that is, usually no more than 20 kelvins above  $T_c$  [50]. Obviously, to obtain information about the PG in the entire temperature range, from  $T^*$  to  $T_G$ , an equation is needed that describes the entire experimental curve  $\sigma'(T)$  and contains the PG parameter  $\Delta^*(T)$  in explicit form. Such an equation was proposed in Ref. [49] taking into account the LP model:

$$\sigma'(T) = \frac{e^2 A_4 (1 - \frac{T}{T^*}) \exp\left(-\frac{\Delta^*}{T}\right)}{16\hbar\xi_c(0)\sqrt{2\varepsilon_{c0}^* \sinh\left(\frac{2\varepsilon}{\varepsilon_{c0}^*}\right)}}. \quad (2)$$

Here  $(1-T/T^*)$  and  $\exp(-\Delta^*/T)$  take into account the dynamics of LPs formation at  $T \leq T^*$  and their destruction by  $kT$  near  $T_c$ , respectively.

Solving Eq. (2) with respect to  $\Delta^*(T)$ , we obtain

$$\Delta^*(T) = T \ln \frac{e^2 A_4 (1 - \frac{T}{T^*})}{\sigma'(T) 16\hbar\xi_c(0)\sqrt{2\varepsilon_{c0}^* \sinh\left(\frac{2\varepsilon}{\varepsilon_{c0}^*}\right)}} \quad (3)$$

where  $\sigma'(T)$  is the experimentally measured excess conductivity over the entire temperature range from  $T^*$  to  $T_G$ . Accordingly,  $A_4$  is a numerical coefficient that has the meaning of the C-factor in the FLC theory,  $\Delta^*(T_G)$  is the value of the PG parameter near  $T_c$  and  $\varepsilon_{c0}^*$  is some specific theoretical parameter that is discussed in detail below [12, 42, 43, 49]. As can be seen, equations (2) and (3) contain a number of parameters that, importantly, can be determined experimentally [12, 49, 50]. Such parameters as  $T^*$ ,  $T_c^{mf}$ , reduced temperature  $\varepsilon = (T - T_c^{mf})/T_c^{mf}$  and  $\xi_c(0)$  at various values of  $B$  have already been determined in our previous paper devoted to the analysis of FLC in the same YBCO film [33] (see Table I).  $T_c^{mf}$  determines reduced temperature and is therefore of primary importance for FLC and PG analysis [12, 43]. In fact,  $T_c^{mf}$  is the mean-field critical temperature, separating the range of SC fluctuations from the critical fluctuations in the region of  $T_c$ , where the SC order parameter  $\Delta < kT$  and Bogolyubov's mean-field theory does not work [51, 52]. To find  $T_c^{mf}$ , we use the fact [12, 38, 47, 50] that in all HTSCs, near  $T_c$ ,  $\sigma'(T)$  is always described by the standard equation of the 3D-AL theory [36], in which  $\sigma'_{AL3D} \sim \varepsilon^{-1/2} \sim (T - T_c^{mf})^{-1/2}$ . Accordingly,  $\sigma'^{-2} \sim (T - T_c^{mf})$  and the intersection of its linear extrapolation with the temperature axis just determines  $T_c^{mf}$ , since  $\sigma'^{-2} = 0$  at  $T = T_c^{mf}$  [43]. Note that always  $T_c^{mf} > T_c$ . The Ginzburg temperature  $T_G > T_c^{mf}$  is another characteristic, down to which the mean-field theory works [53, 54]. The remaining parameters shown in the table are discussed in detail in our previous article [33].

As can be seen from the Table I, the magnetic field affects all characteristic temperatures, except  $T^* = 215$  K, which actually remains unchanged and is not shown. The same conclusions about the independence of  $T^*$  from the magnetic field were obtained both for the YBCO [21] compounds and for the  $\text{Bi}_2\text{Sr}_2\text{CaCu}_2\text{O}_{8+y}$  (Bi-2212) [55, 56] compounds, despite the very strong magnetic fields used in the experiment. These results once again emphasize the

TABLE II:  
Parameters of the pseudogap analysis for  $\text{YBa}_2\text{Cu}_3\text{O}_{7-\delta}$  film depending on the applied magnetic field.

$B$ (T)	$\epsilon_{c0}^*$	$A_4$	$2\Delta^*(T_G)/k_B T_c$	$T_{pair}$ (K)	$\Delta^*(T_{pair})/k_B$ (K)	$\Delta^*(T_G)/k_B$ (K)	$\langle n_{\uparrow} n_{\downarrow} \rangle$
0	0.26	7.7	5.0	140	254	219.5	0.307
0.5	0.28	9.3	5.0	140	254	218.3	0.305
1	0.25	9.65	5.0	140	254	217.8	0.305
2	0.25	15.3	5.0	135	254	215.3	0.301
3	0.25	27.1	5.0	135	254	215.4	0.301
4	0.25	27.8	5.0	135	254	213.4	0.299
5	0.25	28.5	5.0	130	254	211.4	0.296
6	0.25	29.1	5.0	130	254	209.8	0.294
7	0.25	27.7	4.9	130	254	207.2	0.290
8	0.25	28.0	4.9	130	254	203.8	0.285

well-known fact that even a strong magnetic field ( $\sim 80$  T, [21]) does not have a noticeable effect on the resistivity of cuprates in the normal state.

All missing parameters, required for Eq. 2 and 3, such as the theoretical parameter  $\epsilon_{c0}^*$ ,  $\Delta^*(T_G)$  and coefficient  $A_4$  can also be determined from experiment using the approach developed within the LP model [19, 49]. Fig. 3 shows the dependences of  $\ln\sigma'$  on  $\ln\epsilon$  for  $B = 0, 1$  T, 3 T and 8 T over the entire temperature range from  $T^*$  to  $T_G$ . It has been shown theoretically that  $\sigma'^{-1} \sim \exp\epsilon$  in a certain temperature range, indicated by the arrows at  $\ln\epsilon_{c01}$  and  $\ln\epsilon_{c02}$  on the main panels [57]. This feature turns out to be one of the main properties of most HTSCs [12, 19, 49, 50]. As a result, in the interval  $\epsilon_{c01} < \epsilon < \epsilon_{c02}$  (see insets in panels),  $\ln\sigma'^{-1}$  is a linear function of  $\epsilon$  with a slope  $\alpha^*$ , which determines the parameter  $\epsilon_{c0}^* = 1/\alpha^*$  [57]. This approach makes it possible to obtain reliable values of  $\epsilon_{c0}^*$  for all values of applied magnetic field, which are given in Table II. Fig. 4 represents the same dependences for  $B = 0$  T (upper panel) and  $B = 8$  T (lower panel), but in coordinates  $\ln\sigma'$  vs  $1/T$ . As established in Refs. [12, 19, 50], in this case, the PG parameter  $\Delta^*(T_G)$  significantly affects the shape of the theoretical curves presented in Fig. 4, at  $T > T_{01}$ , i.e., noticeably higher than the region of SC fluctuations. Therefore, by selecting the best fit, the correct value of  $\Delta^*(T_G)$  can be determined (Table II). In addition, it was convincingly established that  $\Delta^*(T_G) = \Delta(0)$ , where  $\Delta$  is the SC gap [58, 59]. We emphasize that it is the value  $\Delta^*(T_G)$  that determines the true value of PG and is used to estimate the value of the BCS ratio  $2\Delta(0)/k_B T_c = 2\Delta^*(T_G)/k_B T_c$  in a specific HTSC sample [19, 47, 50]. The best approximation of  $\ln\sigma'$  as a function of  $1/T$  from Eq. (2) for the case  $B = 0$  is achieved at  $2\Delta^*(T_G)/k_B T_c = 5.0 \pm 0.05$  (Table II), which corresponds to the strong coupling limit characteristic of YBCO [60–62].

When  $\epsilon_{c0}^*$  and  $\Delta^*(T_G)$  are known, the coefficient  $A_4$  can be determined by approximating the data  $\sigma'(\epsilon)$  by Eq. (2) and using the found parameters (Tables I, II). With the correct choice of  $A_4$  (Table II), the theory is combined with experiment in the region of 3D AL fluctuation near  $T_c$ , where  $\ln\sigma'(\epsilon)(\ln\epsilon)$  is a linear function of the reduced temperature  $\epsilon$  with slope  $\lambda = -1/2$  [12, 19, 50] (Fig. 3). As can be seen in the figure, Eq. (2) describes well the experiment at temperatures between  $T^*$  and  $T_G$  at  $B = 0$  as well as for all applied magnetic fields. However, it is worth noting that above  $\sim 2.5$  T, in the temperature range from  $T_{c01}$  to  $T_{c02}$  ( $\ln\epsilon_{c01}$  and  $\ln\epsilon_{c02}$  in Fig. 3), the experimental data deviate slightly downward from the theoretical curve. This is most likely due to the fact that at  $B > 2.5$  T the temperature dependence of the FLC changes from 2D MT to 2D AL [33], which is not taken into account in the LP model. At  $B = 0$  (left upper panel), the parameters are  $A_4 = 7.7$ ,  $\epsilon_{c0}^* = 0.26$ , and  $\Delta^*(T_G)/k_B = 219.5$  K (Table II). The values of the corresponding parameters for all magnetic fields are also given in the Tables. As can be seen, all parameters, except  $2\Delta^*(T_c)/k_B T_c$ , change noticeably with a change in the field, which suggests a possible influence of the field on the PG as well.

The fact that all  $\sigma'(T, B)$  are well described by equation (2) (Fig. 3) suggests that equation (3) with the corresponding set of found parameters should give reliable values, as well as temperature and magnetic dependences of the parameter  $\Delta^*(T, B)$  at any applied field. Figure 5 (main panel) shows the result of the  $\Delta^*(T)$  analysis using Eq. (3) for  $B = 0$  and 8 T with all necessary for the PG analysis parameters given in Tables I and II. As expected, at  $B = 0$  (black dots in the figure) the shape of  $\Delta^*(T)$  is typical for YBCO films [19, 49] and untwinned single crystals [38], with a maximum at  $T = T_{pair} \approx 140$  K and a minimum at  $T \approx T_{01}$  [35, 38, 50]. As mentioned above,  $T_{pair}$  is the BEC-BCS crossover temperature [11, 12, 14–17, 49]. Accordingly, as  $T$  approaches  $T_c$ , there is a maximum of

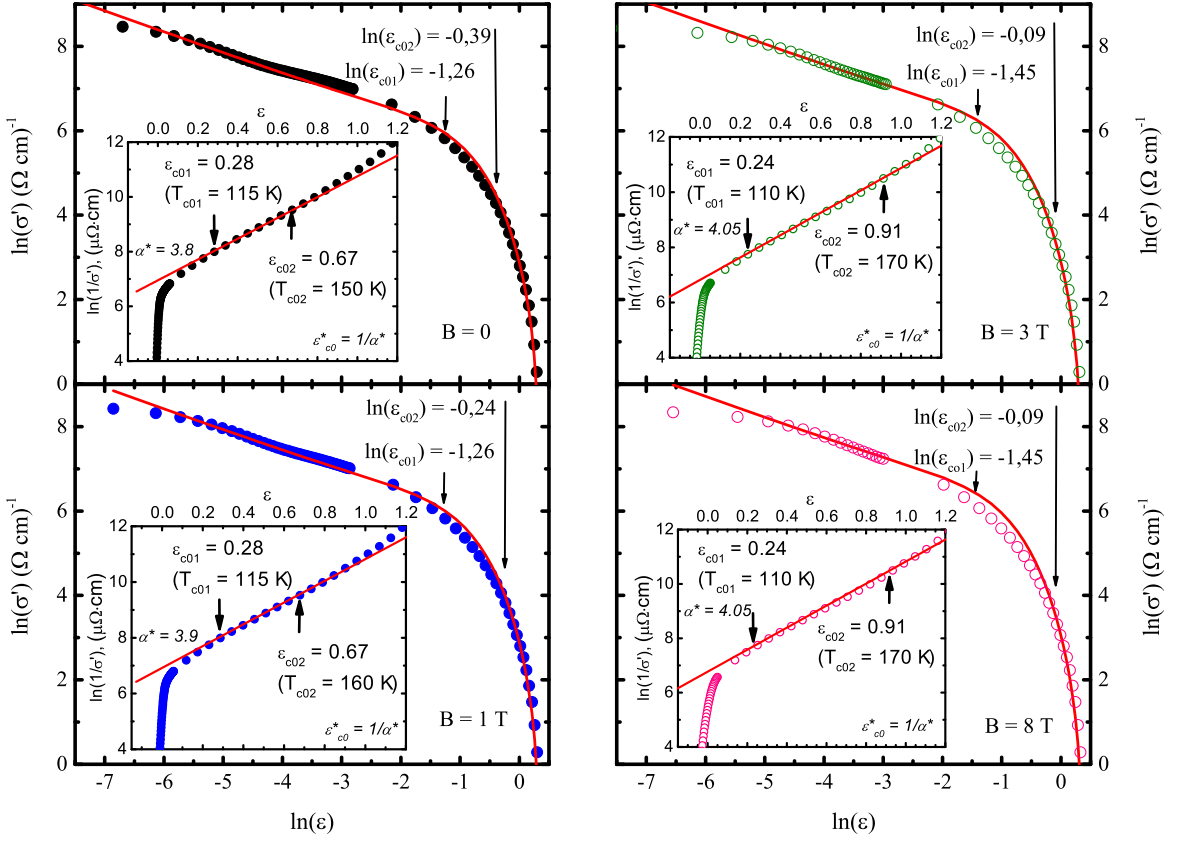


FIG. 3:  $\ln\sigma'$  vs  $\ln\epsilon$  (symbols) plotted in the entire temperature range from  $T^*$  down to  $T_c^{mf}$  for  $B = 0$  (left upper panel), 1 T (left lower panel), 3 T (right upper panel) and 8 T (right lower panel). The red solid curves at each panel are fits to the data with Eq.(2). Insets:  $\ln\sigma'^{-1}$  as a function of  $\epsilon$ . The straight red lines denote the linear parts of the curves between  $\epsilon_{c01}$  to  $\epsilon_{c02}$ . The slope  $\alpha^*$  determines the parameter  $\epsilon_{c0}^* = 1/\alpha^*$  (see text).

$\Delta^*(T)$  just below  $T_0$  and a minimum at  $T = T_G$  [19, 49] (see inset in Fig. 5). Below  $T_G$ , there is usually a sharp jump in  $\Delta^*(T)$  at  $T \rightarrow T_c^{mf}$ , which is deliberately not shown due to its non-physical nature, since it corresponds to the transition to the region of critical fluctuations, where the LP model does not work. Thus, the approach in the framework of the LP model makes it possible to determine the exact values of  $T_G$  and, as a consequence, to obtain reliable values of  $\Delta^*(T_G) \approx \Delta(0)$  [19, 49, 57–59] depending on the applied magnetic field (Table II).

Moreover, the  $\Delta^*(T_G)$  vs  $B$  (Fig.6) can be approximated by two linear sections with the same slope: the first one occurs from 0 to 2 T and the second one, after a plateau between 2 and 3 T, is clearly seen from 3 to 8 T. It should be noted, that the observed behavior of  $\Delta^*(T_G)$  correlates with the FLC change from 2D MT to 2D AL [33], as was already discussed above.

As can be seen from the Fig. 5 (main panel), a magnetic field  $B = 8 \text{ T}$  noticeably reduces the PG values at all temperatures above  $T_{pair}$ , especially near  $T^*$ . This seems quite surprising, since the magnetic field has virtually no effect on the resistivity curve at high temperatures (Fig. 1 and [43, 63]). Thus, our result actually highlights the increased sensitivity of our approach and leads us to the conclusion that the magnetic field has a much stronger effect on local pairs than on normal electrons. However, to explain this very important and somewhat unexpected result, it is also necessary to keep in mind that, in accordance with the LP model [18], the magnetic field, which is relatively weak in our case, does not destroy the SSBs arising in HTSCs at  $T < T^*$  [17]. On the other hand, we must also remember that PG arises simultaneously with a decrease in the density of states (DOS) at the Fermi level

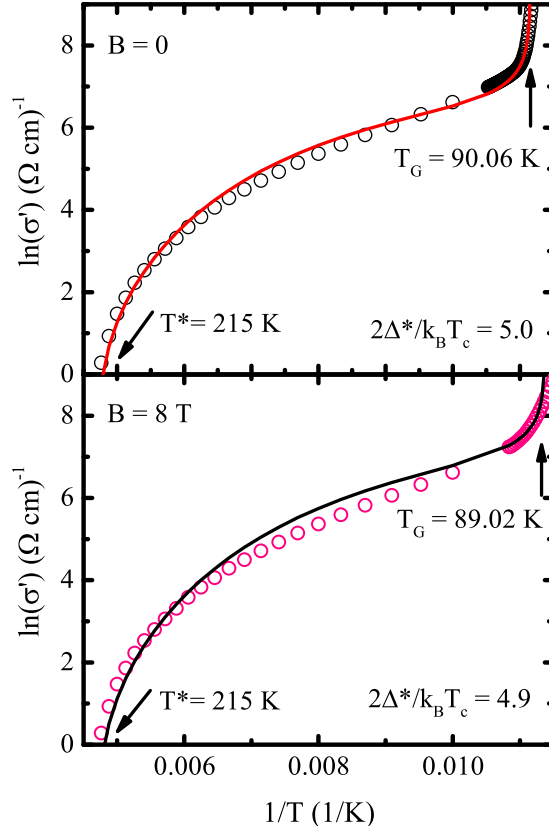


FIG. 4:  $\ln \sigma'$  vs  $1/T$  for  $B = 0$  (upper panel, black circles) and 8 T (lower panel, pink circles) over the entire temperature range from  $T^*$  to  $T_G$ . The solid red and black curves on each panel are fits to the data with Eq. (2). The best fit is obtained when  $2\Delta^*(T_G)/k_B T_c = 5.0 \pm 0.05$  ( $B = 0$ ) and  $2\Delta^*(T_G)/k_B T_c = 4.9 \pm 0.05$  ( $B = 8$  T).

[64, 65]. This means that we can only assume that the magnetic field somehow increases the DOS, thereby leading to the observed decrease in the PG. It is possible that the magnetic field somehow changes the distribution of normal electrons and SBBs in the sample, thereby changing the DOS. However, clarification of this issue requires special research.

From  $T_{pair}$  down to  $T_{01}$  the opposite dynamics is observed (Fig. 5), expressed in a slight increase in  $\Delta^*(T)$ , which is also surprising. Therefore, we can assume that the influence of the magnetic field on the LPs and, possibly, on the DOS below  $T_{pair}$  has also changed. Interestingly, the absolute value of  $\Delta^*(T_{pair})$  remains constant, while  $T_{pair}$  shifts towards low-temperature region from 140 K at  $B = 0$  to 130 K at 8 T. It seems that the entire  $\Delta^*(T)$  curve also shifts towards low temperatures along with the field, which can be considered as another reason for the observed decrease in  $\Delta^*(T)$ . However, measured decrease in  $T_c^{mf}$  is  $\Delta T_c^{mf} = 1.75$  K and  $\Delta T_G$  is only 1.04 K and, strictly speaking, is clearly insufficient to account for the final shape of  $\Delta^*(T)$ .

At the same time, the BCS ratio  $2\Delta^*(T_G)/k_B T_c$  at  $B > 7$  T tends to decrease from 5.0 to 4.9 (Fig. 4 and Table II). Note that all other film parameters, except  $\Delta^*(T_{pair}) = 254$  K, also change noticeably (Table II). Our analysis of Eq. (3) showed that it is the change in the film parameters that leads to the observed unexpected  $\Delta^*(T)$  at  $B = 8$  T, since the value of the excess conductivity  $\sigma'(T)$  is considered to be the same as at  $B = 0$ . But, strictly speaking, the physics of the change in the shape of PG under the influence of a magnetic field remains unclear.

As  $T$  approaches  $T_c$ , the magnetic field begins to intensively reduce  $\Delta^*(T)$  in the region of SC fluctuations below  $T_{01}(B = 0) = 100$  K (see inset in Fig. 5), while in a certain temperature range up to  $T_{pair}(B = 8$  T) = 103 K the  $\Delta^*(T)$  remains increased. The evolution of  $\Delta^*(T)$  below  $T_{01}$  with increasing magnetic field is as follows (see inset in Fig. 5). The sharp low-temperature maximum near  $T_0$  is suppressed in magnitude and shifts toward higher temperatures and completely disappears at  $B > 5$  T. At the same time, starting from  $\sim 0.5$  T, above  $T_G$  a pronounced minimum

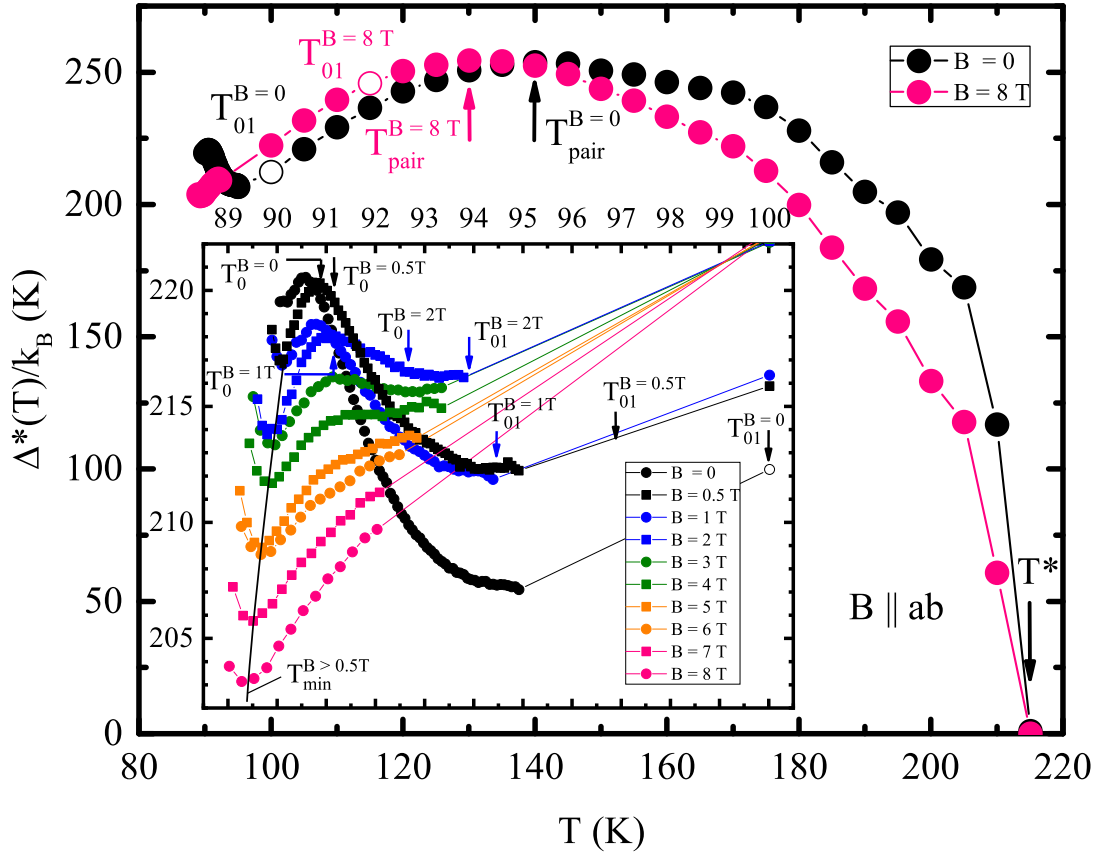


FIG. 5:  $\Delta^*(T)$  as a function of  $T$  of the studied  $\text{YBa}_2\text{Cu}_3\text{O}_{7-\delta}$  film, calculated by Eq. (3) for  $B = 0$  (black dots) and 8 T (pink dots). Empty circles indicate the characteristic temperature  $T_{01}$ , which limits the range of SC fluctuations from above (also in the inset for  $B = 0$ ). Inset: The same dependences for the temperature interval  $T_G < T < T_{01}$  for  $B = 0, 0.5, 1, 2, 3, 4, 5, 6, 7$  and 8 T. The scales in the inset have the same dimensions as the main figure. All characteristic temperatures, both on the main panel and in the inset, are indicated by arrows. The leftmost symbol of each curve is  $T_G$  that limits SC fluctuations from below. The auxiliary black curve in the inset helps to trace the field evolution of the low temperature minimum  $T_{min}$  that appears at  $B > 0.5$  T. The other solid curves are drawn to guide the eyes.

appears at  $T_{min}$ . As can be seen in the inset, both  $\Delta^*(T_{min})$  and, more importantly,  $\Delta^*(T_G)$ , which is the leftmost point of each curve, decrease noticeably with increasing field, simultaneously shifting towards lower temperatures. It is very likely that this is due to the pair-breaking effect of the magnetic field on the FCPs, leading to the appearance of noticeable magnetoresistance, as well as the possible influence of the two-dimensional vortex lattice created by the magnetic field, which is discussed in [33]. However, from Fig. 6 it can be seen that the decrease in  $\Delta^*(T_G)$  with increasing field is also unusual. Indeed, the  $\Delta^*(T_G)$  dependence consists of two linear sections with the same slope, but shifted by  $\sim 1$  T at  $B > 2$  T. It should be noted, that the observed behavior of  $\Delta^*(T_G)$  correlates with the change in FLC from the 3D-AL to 2D-MT [33], as discussed above. The revealed behavior also correlates with the fact that all characteristic temperatures detected in the analysis of FLC, as well as the range of SC fluctuations  $\Delta T_{fl}$  and the coherence length along the  $c$  axis  $\xi_c(0)$  increase sharply at  $B \geq 3$  T (Table I and [33]). All these results suggest that pair breaking is not the only factor in the influence of the magnetic field.

The pair-breaking effect of the magnetic field should lead to a decrease in the density of FCPs. To clarify this issue, we compare the pseudogap parameters  $\Delta^*(T)/\Delta^*_{max}$ , calculated for all applied fields near  $T_c$ , with the Peters-Bauer (PB) theory [39]. In the theory, within the framework of the three-dimensional attractive Hubbard model,

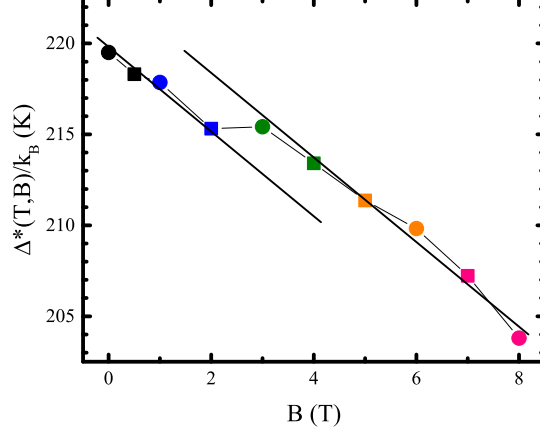


FIG. 6:  $\Delta^*(T_G)$  as a function of  $B$ , showing a fairly good linear relationship, indicated by two dashed lines shifted by 1 T at  $B > 2$  T. The thin solid line is drawn to guide the eyes.

the temperature dependences of the local density  $\langle n_{\uparrow}n_{\downarrow} \rangle$  of pairs in HTSCs are calculated for various temperatures  $T/W$ , interactions  $U/W$  and filling factors. In this case,  $U$  is the activation energy and  $W$  is the band width. For all cuprates, the shape  $\Delta^*(T)$  near  $T_c$ , with a maximum near  $T_0$  followed by a minimum at  $T_G$  [50] (see Fig. 12 in [50] and Fig. 7 in [35]), resembles the shape of theoretical  $\langle n_{\uparrow}n_{\downarrow} \rangle$  curves at low  $T/W$  and  $U/W$  [39]. This gives every reason to compare experiment with the theory.

The comparison results are shown in Fig. 7. Symbols are the experimental data near  $T_c$  for  $B = 0, 0.5, 1, 2$  and 8 T. The solid black curve corresponds to the theoretical dependence of  $\langle n_{\uparrow}n_{\downarrow} \rangle$  on  $T/W$  at  $U/W = 0.2$ . The dashed lines indicate the temperatures  $T_0$  and  $T_G$ . To carry out the analysis, the minimum  $\Delta^*(T)/\Delta^*_{max}$  at  $T_G$ , measured at  $B = 0$ , is combined with the  $T_G$  line, and the corresponding value  $\Delta^*(T)/\Delta^*_{max}$  at  $T_0$  is combined with the  $T_0$  line and then the result is compared with each theoretical curve calculated at different  $U/W$  values. The best fit is obtained with a  $U/W = 0.2$  curve, indicating that in this case  $\langle n_{\uparrow}n_{\downarrow} \rangle \sim 0.3$ , which is a typical value for various HTSCs at  $B = 0$  [38, 66, 67]. In this case, the data fits the theoretical curve over the largest temperature range above the maximum, as shown in the figure. This approach allows us to find the approximation coefficients both along the X and Y axis, which are then used at all values of the magnetic field.

As can be seen in Fig. 7, with an increase in the magnetic field, the data at higher  $T$  noticeably deviate from the theory upward, and at  $B = 8$  T the data points (pink) do not fit the theoretical curve at all. But more importantly, as the field increases, the value of  $\Delta^*(T)/\Delta^*_{max} = \langle n_{\uparrow}n_{\downarrow} \rangle \approx 0.307$  at  $B = 0$  drops to  $\langle n_{\uparrow}n_{\downarrow} \rangle \approx 0.285$  at  $B = 8$  T. Simple algebra yields a reduction in local pair density of about 7.0 %. However, if we now take the data shown in the inset to Fig. 5, we will see that  $\Delta^*(T) \approx 219$  K at  $B = 0$  and  $\Delta^*(T) \sim 204$  K at  $B = 8$  T, that is, under the influence of the field,  $\Delta^*(T)$  decreases by approximately the same 7.0 %. Thus, we can conclude that near  $T_c$ , where the LPs turn into FCPs, pair breaking by the magnetic field does play a significant role in reducing PG. But the evolution of the shape of  $\Delta^*(T)$  near  $T_c$  under the influence of a magnetic field (Fig. 5) is most likely determined precisely by the dynamics of the vortices created by the field in the range of SC fluctuations and very likely through some other mechanisms [33].

## Conclusion

For the first time, within the framework of a local pair model, the evolution of the temperature dependence of the pseudogap  $\Delta^*(T)$  in  $\text{YBa}_2\text{Cu}_3\text{O}_{7-\delta}$  film with  $T_c = 88.7$  K under the influence of a magnetic field  $B$  up to 8 T was studied in detail. As expected, at  $B = 0$ ,  $\Delta^*(T)$  in the entire temperature range from the pseudogap opening temperature  $T^*$  to  $T_G$ , down to which the mean field theory works, has a wide maximum at the BEC-BCS transition temperature  $T_{pair} \sim 140$  K, which is typical for well-structured films and non-twinned single crystals. Interestingly, despite the fact that the magnetic field does not affect  $\rho(T)$  at high temperatures, all sample parameters presented in the Tables change noticeably when the field increases to 8 T. This leads to a noticeable change in the shape of  $\Delta^*(T)$ , despite the fact that  $T^*$  and excess conductivity are considered unchanged. A shift in the temperature of the BEC-BCS crossover  $T_{pair}$  to the low temperature region from 140 K at  $B = 0$  to 130 K at 8 T was detected, while

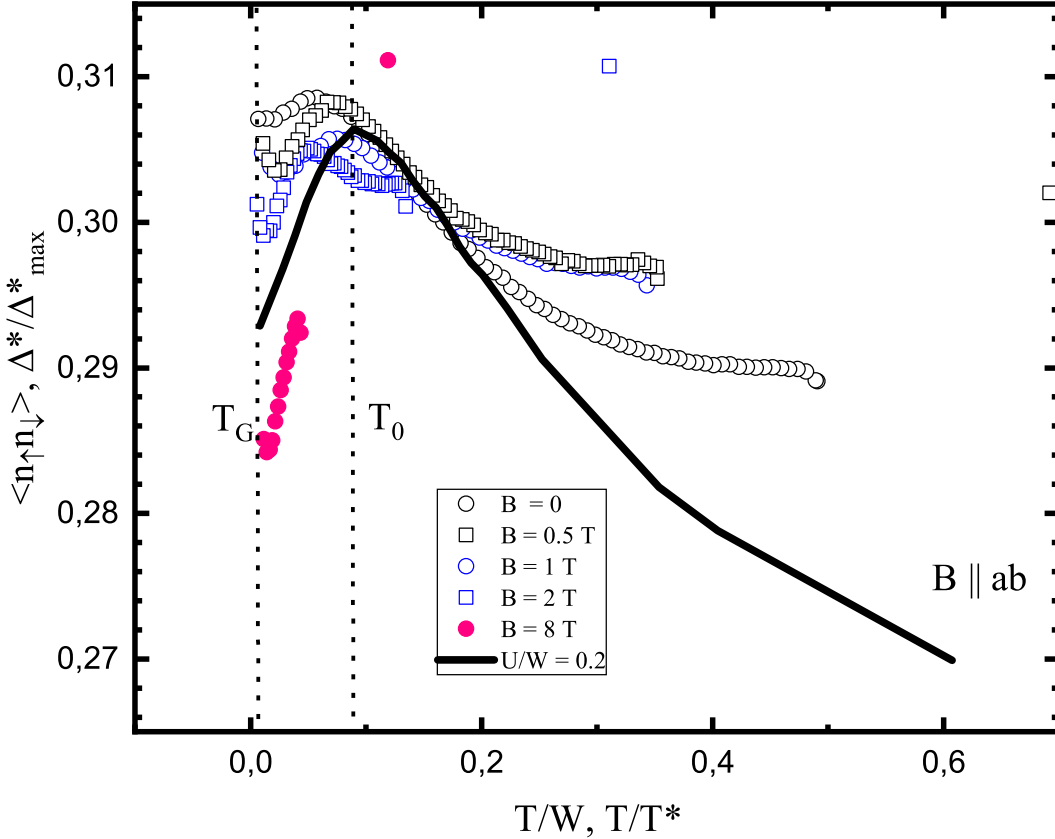


FIG. 7:  $\Delta^*(T)/\Delta_{max}^*$  as functions of  $T/T^*$  near  $T_c$  for the magnetic fields  $B = 0$  (black circles), 0.5 (black squares), 1 (blue circles), 2 (blue squares) and 8 T (pink dots) compared with the theoretical dependence of  $\langle n_{\uparrow}n_{\downarrow} \rangle$  on  $T/W$  at  $U/W = 0.2$  (black curve). The dashed lines indicate the temperatures  $T_0$  and  $T_G$ .

the maximum value  $\Delta^*(T_{pair})$  is maintained regardless of  $B$ . It looks like the entire  $\Delta^*(T)$  curve is somehow shifting towards lower temperatures. The text discusses some attempts to describe the found behavior of  $\Delta^*(T)$ , but, fairly speaking, the reason for the unusual effect observed remains unclear.

In the region of SC fluctuations near  $T_c$  the magnetic field begins to intensively reduce  $\Delta^*(T)$ . The sharp low-temperature maximum near  $T_0$  is gradually suppressed, shifts toward higher temperatures and completely disappears at  $B > 5$  T. At the same time, starting from  $\sim 0.5$  T, above  $T_G$ , a pronounced minimum appears at  $T_{min}$ . At the same time, both  $\Delta^*(T_G)$ , which is the leftmost point of each curve, and  $\Delta^*(T_{min})$  decrease noticeably with increasing field, simultaneously shifting towards lower temperatures. The decrease in  $\Delta^*(T_G)$  with increasing field turns out to be also unusual. Indeed, the  $\Delta^*(T_G)$  dependence consists of two linear sections with the same slope, but shifted by  $\sim 1$  T at  $B > 2$  T. The revealed behavior also correlates with changes in several other sample parameters at  $B \geq 3$  T, suggesting that pair breaking is not the only factor in the influence of the magnetic field.

The comparison of the data with the Peters-Bauer theory has shown that near  $T_c$ , where the local pairs are transformed into fluctuating Cooper pairs, pair breaking by the magnetic field does play a significant role in reducing PG. But the specific evolution of the shape  $\Delta^*(T)$ , discovered near  $T_c$  under the influence of a magnetic field, is most likely determined precisely by the influence of the two-dimensional vortex lattice created by the magnetic field, and also, probably, by some other mechanisms that prevent the formation of superconducting fluctuations near  $T_c$ .

### Acknowledgements

The work was supported by the National Academy of Sciences of Ukraine within the F19-5 project.

We also acknowledge support from the European Federation of Academies of Sciences and Humanities (ALLEA) through Grant EFDS-FL1-32 (A.L.S.). A.L.S. also thanks the Division of Low Temperatures and Superconductivity, INTiBS Wrocław, Poland, for their hospitality. Work was partly funded by Research Council of Finland, project No. 343309.

- 
- [1] S. Lee, J.-H. Kim, Y.-W. Kwon, [arXiv:2307.12008](https://arxiv.org/abs/2307.12008) (2023).
- [2] D. Garisto, *Nature* **620**, 705 (2023).
- [3] P. Puphal, M. Y. P. Akbar, M. Hepting, E. Goering, M. Isobe, A. A. Nugroho, B. Keimer, [arXiv:2308.06256](https://arxiv.org/abs/2308.06256) (2023).
- [4] A. A. Kordyuk, *Low Temp. Phys.* **41**, 319 (2015).
- [5] J. Gao, J. W. Park, K. Kim, S. K. Song, H. R. Park, J. Lee, J. Park, F. Chen, X. Luo, Y. Sun, and H. W. Yeom, *Nano. Lett.* **20**, 6299-6305 (2020).
- [6] J. L. Tallon, J. G. Storey, J. R. Cooper, and J. W. Loram, *Phys. Rev. B* **101**, 174512 (2020).
- [7] Y. Y. Peng, R. Fumagalli, Y. Ding, M. Minola, S. Caprara, D. Betto, M. Bluschke, G. M. De Luca, K. Kummer, E. Lefrançois, M. Salluzzo, H. Suzuki, M. Le Tacon, X. J. Zhou, N. B. Brookes, B. Keimer, L. Braicovich, M. Grilli, and G. Ghiringhelli, *Nat. Mater.* **17**, 697 (2018).
- [8] D. Chakraborty, M. Grandadam, M. Y. Hamidian, J. C. S. Davis, Y. Sidis, and C. Pépin, *Phys. Rev. B* **100**, 224511 (2019).
- [9] I. Esterlis, S. A. Kivelson, and D. J. Scalapino, *Phys. Rev. B* **99**, 174516 (2019).
- [10] G. Yu, D.-D. Xia, D. Pelc, R.-H. He, N.-H. Kaneko, T. Sasagawa, Y. Li, X. Zhao, N. Barisic, A. Shekhter, and M. Greven, *Phys. Rev. B* **99**, 214502 (2019).
- [11] V. M. Loktev, R. M. Quick, and S. G. Sharapov, *Phys. Rep.* **349**, 1 (2001).
- [12] A. L. Solovjov, *Pseudogap and local pairs in high- $T_c$  superconductors*, in: *Superconductors-Materials, Properties and Applications*, A. Gabovich (ed.), InTech, Rijeka (2012), Chap. 7, p. 137.
- [13] R. Haussmann, *Phys. Rev. B* **49**, 12975 (1994).
- [14] O. Tchernyshyov, *Phys. Rev. B* **56**, 3372 (1997).
- [15] J. R. Engelbrecht, A. Nazarenko, M. Randeria, and E. Dagotto, *Phys. Rev. B* **57**, 13406 (1998).
- [16] V. J. Emery and S. A. Kivelson, *Nature* **374**, 434 (1995).
- [17] M. Randeria, *Nat. Phys.* **6**, 561 (2010).
- [18] A. L. Solovjov and K. Rogacki, *Low Temp. Phys.* **49**, 375 (2023).
- [19] A. L. Solovjov, V. M. Dmitriev, *Low Temp. Phys.* **35**, 169 (2009).
- [20] B. P. Stojković, and D. Pines, *Phys. Rev. B* **55**, 8576 (1997).
- [21] S. Badoux et al., *Nature (London)* **531**, 210 (2016).
- [22] A. M. Gabovich and A. I. Voitenko, *Low Temp. Phys.* **42**, 1103 (2016).
- [23] L. Taillefer, *Annu. Rev. Condens. Matter Phys.* **1**, 51 (2010).
- [24] S. Dzhumanov, U.T. Kurbanov *Modern Physics Letters B* **32**, 1850312 (2018).
- [25] S. Dzhumanov, U.T. Kurbanov *Superlattices and Microstructures* **84**, 66 (2015).
- [26] S. Wang, P. Choubey, Y. X. Chong, W. Chen, W. Ren, H. Eisaki, S. Uchida, P. J. Hirschfeld and J. C. S. Davis, *Nature Com.* **12**, 6087 (2021).
- [27] S. F. Kivelson, and S. Lederer, *PNAS* **116**, 14395 (2019).
- [28] N. J. Robinson, P. D. Johnson, T. M. Rice, and A. M. Tsvelik, *Rep. Prog. Phys.* **82**, 126501 (2019).
- [29] V. Mishra, U. Chatterjee, J.C. Campuzano, and M.R. Norman, *Nat. Phys.* **10**, 357 (2014).
- [30] R. V. Vovk, Z. F. Nazyrov, G. Ya. Khadzhai, V. M. Pinto Simoes, V. V. Kruglyak, *Functional Materials* **20**, 208 (2013).
- [31] B. A. Malik, G. H. Rather, K. Asokan, M. A. Malik, *Applied Physics A* **127** (2021).
- [32] R. I. Rey, C. Carballeira, J. M. Doval, J. Mosqueira, M. V. Ramallo, A. Ramos-Álvarez, D. Sónora1, J. A. Veira, J. C. Verde and F. Vidal, *Supercond. Sci. Technol.* **32**, 045009 (2019).
- [33] E. V. Petrenko, L. V. Omelchenko, Yu. A. Kolesnichenko, N. V. Shytov, K. Rogacki, D. M. Sergeev, and A. L. Solovjov, *Low Temp. Phys.* **47**, 1148 (2021).
- [34] P. G. De Gennes, *Superconductivity of Metals and Alloys* W. A. Benjamin, Inc., New York, Amsterdam (1968) p. 280.
- [35] A. L. Solovjov, L. V. Omelchenko, R. V. Vovk, O. V. Dobrovolskiy, S. N. Kamchatnaya, D. M. Sergeev, *Curr. Appl. Phys.* **16**, 931 (2016).
- [36] L. G. Aslamazov and A. L. Larkin, *Phys. Lett. A* **26**, 238 (1968).
- [37] S. Hikami and A. I. Larkin, *Mod. Phys. Lett. B* **2**, 693 (1988).
- [38] A. L. Solovjov, E. V. Petrenko, L. V. Omelchenko, R. V. Vovk, I. L. Goulatis, and A. Chroneos, *Sci. Rep.* **9**, 9274 (2019).
- [39] R. Peters and J. Bauer, *Phys. Rev. B* **92**, 014511 (2015).
- [40] P. Przyszlupski, I. Komissarov, W. Paszkowicz, P. Dłuzewski, R. Minikayev, M. Sawicki, *J. Appl. Phys.* **95**, 2906 (2004).
- [41] E. V. L. de Mello, M. T. D. Orlando, J. L. Gonzalez, E. S. Caixeiro, and E. Baggio-Saitovich, *Phys. Rev. B* **66**, 092504 (2002).

- [42] A. L. Solovjov, H. - U. Habermeier, T. Haage, *Low Temp. Phys.* **28**, 144 (2002).
- [43] B. Oh, K. Char, A. D. Kent, M. Naito, M. R. Beasley, T. H. Geballe, R. H. Hammond, A. Kapitulnik, and J. M. Graybeal, *Phys. Rev. B* **37**, 7861 (1988).
- [44] E. Nazarova, A. Zaleski, K. Buchkov, *Physica C* **470**, 421 (2010).
- [45] Y. V. Pustovit and A. A. Kordyuk, *Fiz. Nizk. Temp.* **42**, 1268 (2016) [*Low Temp. Phys.* **42**, 995 (2016)].
- [46] W. Lang, G. Heine, P. Schwab, X. Z. Wang, and D. Bauerle, *Phys. Rev. B* **49**, 4209 (1994).
- [47] A. L. Solovjov, L. V. Omelchenko, R. V. Vovk, O. V. Dobrovolskiy, Z. F. Nazzyrov, S. N. Kamchatnaya, and D. M. Sergeyev, *Physica B* **493**, 58 (2016).
- [48] Y. Ando, S. Komiya, K. Segawa, S. Ono, and Y. Kurita, *Phys. Rev. Lett.* **93**, 267001 (2004).
- [49] A. L. Solovjov and V. M. Dmitriev, *Fiz. Nizk. Temp.* **32**, 139 (2006) [*Low Temp. Phys.* **32**, 99 (2006)].
- [50] A. L. Solovjov, L. V. Omelchenko, V. B. Stepanov, R. V. Vovk, H.-U. Habermeier, H. Lochmajer, P. Przyslupski, and K. Rogacki, *Phys. Rev. B* **94**, 224505 (2016).
- [51] V. L. Ginzburg and L. D. Landau, "On the theory of superconductivity", in *On Superconductivity and Superfluidity* (Springer, Berlin, Heidelberg, 2009).
- [52] E. M. Lifshitz and L. P. Pitaevski, *Statistical Physics* (Nauka, Moscow, 1978).
- [53] A. Kapitulnik, M. R. Beasley, C. Castellani, and C. Di Castro, *Phys. Rev. B* **37**, 537 (1988).
- [54] T. Schneider and J. M. Singer, *Phase Transition Approach to High-Temperature Superconductivity: Universal Properties of Cuprate Superconductors* (Imperial College Press, London, 2000).
- [55] P. Pieri, G. C. Strinati, and D. Moroni, *Phys. Rev. Lett.* **89**, 127003 (2002).
- [56] T. Shibauchi, L. Krusin-Elbaum, Ming Li, M. P. Maley, and P. H. Kes, *Phys. Rev. Lett.* **86**, 5763 (2001).
- [57] B. Leridon, A. Defossez, J. Dumont, J. Lesueur, and J. P. Contour, *Phys. Rev. Lett.* **87**, 197007 (2001).
- [58] Y. Yamada, K. Anagawa, T. Shibauchi, T. Fujii, T. Watanabe, A. Matsuda, and M. Suzuki, *Phys. Rev. B* **68**, 054533 (2003).
- [59] J. Stajic, A. Iyengar, K. Levin, B. R. Boyce, and T. R. Lemberger, *Phys. Rev. B* **68**, 024520 (2003).
- [60] D. S. Inosov, J. T. Park, A. Charnukha, Y. Li, A. V. Boris, B. Keimer, and V. Hinkov, *Phys. Rev. B* **83**, 214520 (2011).
- [61] Ø. Fischer, M. Kugler, I. Maggio-Aprile, and C. Berthod, *Rev. Mod. Phys.* **79**, 353 (2007).
- [62] A. I. D'yachenko, V. Y. Tarenkov, V. V. Kononenko, E. M. Rudenko, *Metallofiz. Noveishie Tekhnol.* **38**, 565 (2016).
- [63] Y. Matsuda, T. Hirai, S. Komiya, T. Terashima, Y. Bando, K. Iijima, K. Yamamoto, and K. Hirata, *Phys. Rev. B* **40**, 5176 (1989).
- [64] H. Alloul, F. Rullier-Albenque, B. Vignolle, D. Colson, and A. Forget, *EPL* **91**, 37005 (2010).
- [65] T. Kondo, A. D. Palczewski, Yoichiro Hamaya, T. Takeuchi, J. S. Wen, Z. J. Xu, G. Gu, and A. Kaminski, *Phys. Rev. Lett.* **111**, 157003 (2013).
- [66] A. L. Solovjov, E. V. Petrenko, L. V. Omelchenko, E. Nazarova, K. Buchkov, and K. Rogacki, *Fiz. Nizk. Temp.* **46**, 638 (2020) [*Low. Temp. Phys.* **46**, 538 (2020)].
- [67] A. L. Solovjov, L. V. Omelchenko, E. V. Petrenko, Yu. A. Kolesnichenko, A. S. Kolesnik, S. Dzhumanov, and R. V. Vovk, *Low. Temp. Phys.* **49**, 115 (2023).